Archaeological Prospection
Archaeol. Prospect. **20**, 71–78 (2013)
Published online in Wiley Online Library
(wileyonlinelibrary.com) DOI: 10.1002/arp.1452

Editorial

Satellite Synthetic Aperture Radar in Archaeology and Cultural Landscape: An Overview

Introduction

The availability of very high resolution (VHR) synthetic aperture radar (SAR) data, such as TerraSAR-X and Cosmo Sky Med launched in 2007, opened a new era in spaceborne SAR remote sensing, including archaeology remote sensing. They provide powerful tools, based on active sensors from space operating in the microwave frequency range, which are useful to extract information about the contemporary landscape and make it possible, in some conditions, to infer changes in the former environment and to detect archaeological remains. The availability of VHR active and passive satellite data has grown so rapidly that new problems have arisen, linked mainly to methodological aspects of data analysis and interpretation. Compared with optical images, SAR data processing is characterized by higher complexity. This is particularly evident for archaeological purposes, which historically was limited by the low spatial resolution of early sensors. Despite this drawback, early applications of SAR in archaeology date back to the 1980s and undoubtedly enabled numerous important discoveries and provided new insights in vast deserted areas, as in the case of the Sahara (El-Baz *et al.*, 2007). Nevertheless, these early applications from both aerial and space platforms were mainly demonstrative experimentations made by National Aeronautics and Space Administration (NASA) researchers; but archaeological investigations based on spaceborne SAR were limited to 'operative' applications due to the scarce public availability of data and also due to the complexity of data processing and software. Today the use of satellite SAR in archaeology is still in its experimental stage, even though it undoubtedly offers great potential for manifold applications ranging from the detection of features and sites, to reconstruction of palaeolandscapes and enhancement and preservation of archaeological remains. The current worldwide availability of commercial VHR satellite SAR, along with numerous data processing tools offered by a number of commercial image processing (PCI, EVI) and open source softwares, now makes the use of these data easier and more affordable.

The VHR SAR data can provide a major contribution to overcome limits of passive optical data; being active sensors they are able to 'see through' clouds and dusty conditions, to sense a target at any time of day or night, and, to some extent, 'penetrate' vegetation and soil depending on sensor bands, surface characteristics (ice, desert sand, close canopy, etc.) and conditions (moisture content).

The main critical aspect today, especially for archaeology and cultural landscapes, is that there is still a lack of correspondence between the great amount of spaceborne SAR data and effective methods to extract information linked to traces of past human activity. The main challenges to be addressed in the future are: setting up of systematic investigations in different geographical areas, environments and land cover; the development of effective and user friendly tools to extract subtle cultural features and patterns; and the definition of protocols for supporting a widespread use of satellite SAR in archaeology.

The importance of satellite SAR in archaeology and palaeolandscape studies

Compared with passive optical data, SAR offers a number of advantages, among which, as all-weather imaging tools, they can operate night and day and are less influenced by atmospheric effects. The rationale of using SAR in archaeology is that different surfaces and features exhibit different scattering characteristics and, therefore,

on the basis of the given SAR observation parameters, the backscattering coefficient provides information about surface characteristics, such as roughness, geometric shape and dielectric properties. The most relevant SAR observation parameters include: (i) wavelength range (band), (ii) polarization and (iii) incidence angle. For additional information see, for example, http://earth.esa.int/applications/data_util/SARDOCS/spaceborne/SAR_Courses/SAR_Course_II/parameters_affecting.htm. Here we briefly summarize the potential and limitations of SAR observation parameters for archaeology.

Frequency

Synthetic aperture radars are active sensors operating in the microwave electromagnetic (EM) range, which traditionally is denoted by the letters shown in Table 1. As for optical imaging the frequency is selected according to the mission aims, target and phenomena under investigation. Different frequencies are characterized by different 'penetration capabilities' as shown in Figure 1. From a theoretical point of view, according to basic physical principals, the signal is backscattered by a target with a geometrical dimension comparable with the frequency, and therefore, higher frequencies exhibit greater penetration capabilities. Moreover, for a given frequency the 'real' penetration capability into the soil is linked to a number of factors. Among them the most relevant are: presence/absence of vegetation, moisture content and soil porosity. Actually, the penetration capability is strongly limited by surface characteristics and significantly by moisture content. This is the main reason why early applications of satellite SAR were focused on desert areas.

Nowadays, multifrequency, multisensor and multitemporal data sets are available and they can be used alone or integrated with optical imagery, geophysics and ancillary data (such as meteorological records), to conduct investigations over diverse geographical regions, land cover and varying moisture content. This way we can assess limits and capabilities of SAR performance for archaeology, focusing mainly on the polarization and/or the penetration capability in different conditions.

Polarization

Polarization indicates the orientation of the electric field of an EM wave. Imaging SARs can have different polarization configurations. The most commonly used are the linear polarizations indicated as HH, VV, HV and VH (see Table 2) where the first term refers to the emitted radiation and the latter to the received radiation. The SAR systems can have different polarization levels:

- single polarization – HH or VV or HV or VH
- dual polarization – HH and HV, VV and VH, or HH and VV
- four polarizations – HH, VV, HV, and VH.

The acquisition mode HV or VH are termed cross-polarization, whereas HH and VV mode are denoted as standard polarization. Quadrupole polarization (i.e. polarimetric) SAR provides the four polarizations HH, VV, HV and VH, and also measures the difference in the magnitudes and phase between channels.

Fully polarimetric sensors provide images that can be created using all possible combinations of transmitting and receiving orientations, not just the standard HH and VV (Evans *et al*., 1988; Boerner *et al*., 1998). Polarimetric information plays an important role for data processing and interpretation, as it can improve information extraction relating to: (i) target shape and orientation, (ii) different layering and (iii) diverse moisture content (VV polarization enhances moisture response). The polarization state of an EM wave

Table 1. SAR bands and frequencies.

Name	Nominal frequency range	Wavelength range	Specific bands used in SARs
VHF	30–300 MHz	10–1 m	138–144 MHz, 216–225 MHz
P (UHF)	300–1000 Mhz	100–30 cm	420–450 MHz, 890–942 MHz
L	1–2 GHz	30–15 cm	1.215–1.4 GHz
S	2–4 GHz	17–7.5 cm	2.3–2.5 GHz, 2.7–3.7 GHz
C	4–8 GHz	7.5–3.75 cm	5.25–5.925 GHz
X	8–12 GHz	3.75–2.5 cm	8.5–10–68 GHz
Ku	12–18 GHz	2.5–1.67 cm	13.4–14.0 GHz, 15.7–17.7 GHz
K	18–27 GHz	1.67–1.11 cm	24.05–24.25 GHz
Ka	27–40 GHz	1.11–0.75 cm	33.4–36.0 GHz
V	40–75 GHz	0.75–0.40 cm	59–64 GHz
W	75–110 GHz	0.40–0.27 cm	76–81 GHz 92–100 GHz
Millimetre	110–300 GHz	2.7–1.0 mm	

DOI: 10.1002/arp

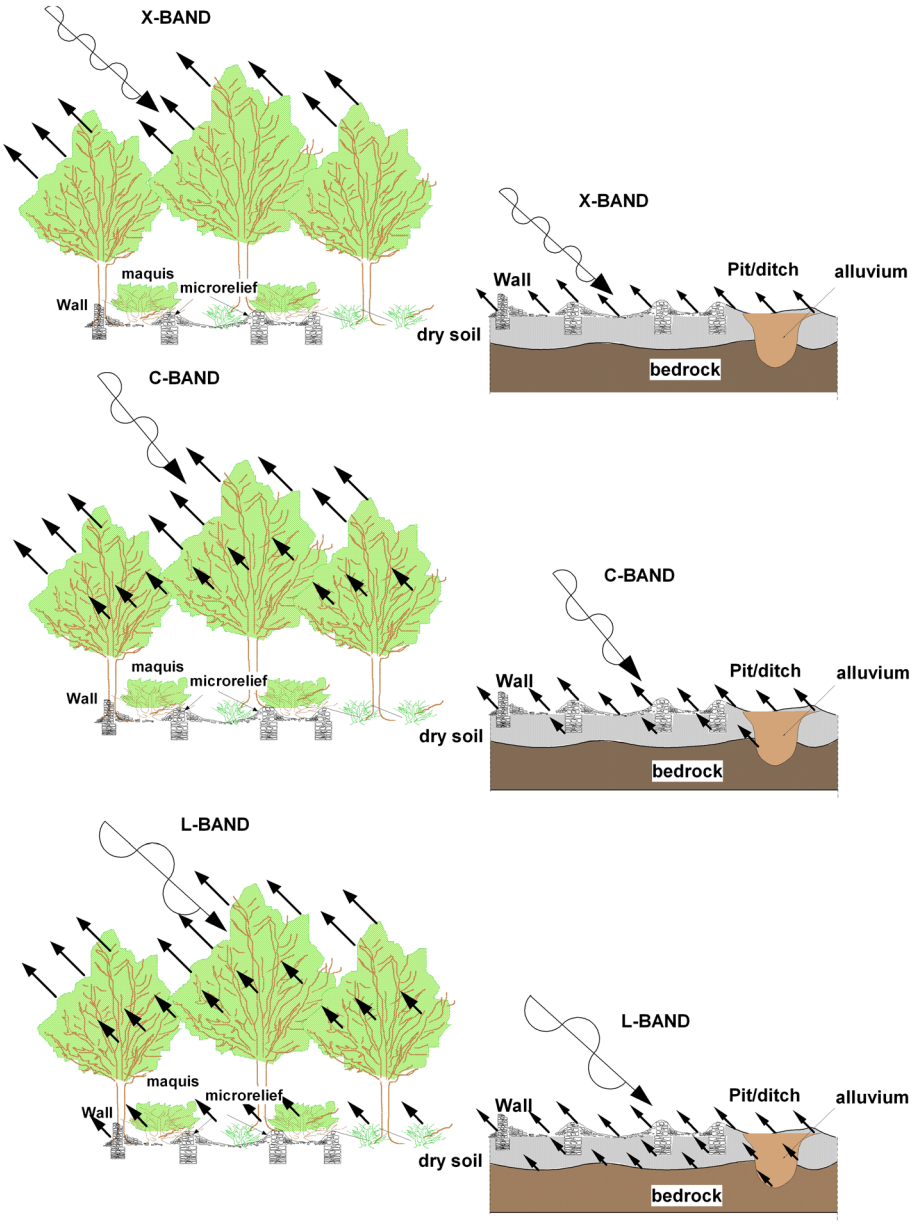

Figure 1. Different penetration capability of SAR according to bands, land cover and surface characteristics.

changes when it strikes an object, or is scattered by a surface or passes through one medium to another. Differences in the backscatter of targets at different polarizations of the incident wave depend (and in turn can inform us) on the geometrical structure and orientation of the target as well as on its geophysical properties.

The amount of backscattered energy depends on the target as well as on the relative orientation of the incident electric field. The polarization state can be expressed mathematically as a combination of transmitted and received polarizations, for each pixel of the polarimetric SAR image. Polarimetric information is, as a first approximation, modelled and stored in a 2×2 coherent backscattering or Sinclair matrix (Boerner *et al.*, 1998). Elements of this matrix describe the relationship between the transmitted and received signal for each pixel at any polarization.

In order to extract information from the polarized backscatter and obtain physical interpretation related to target characteristics, a number of mathematical and physical models have been devised over the years (see e.g. (Freeman and Durden, 1992; Freeman and

DOI: 10.1002/arp

Table 2. SAR system parameters.

SAR system	Band	Polarization	Incident angle (°)	Resolution (mt)	Swath width (km)	Organization	Altitude (km)	Orbit inclination (°)	Launch year
SEA-SAT	L	HH	23	25	100	NASA	790	108	1978
SIR-A	L	HH	45	30	50	NASA	225	57	1981
SIR-B	L	HH	20–60	30	50	NASA	225	57	1984
ALMAZ-1	S	HH	30–60	15	20–45	RSA (PKA)	300	72.7	1991
ERS-1	C	VV	24	25	100	ESA	790	97.7	1991
JERS-1	L	HH	35	18	76	NSDA/MITI	568	97.7	1992
SIR-C	C,L	All	17–60	25	15–100	NASA	225	57	1994
X-SAR	X	VV	17–60	25	15–40	DLR/ASI	228	57	1994
ERS-2	C	HH	24	25	100	ESA	785	97.7	1995
SAR-SAT	C	HH	17–50	10–100	50–170	CSA	790	98.6	1995
PRIRODA	S,L	HH	35	30	120	RSA/DLR	394	51.6	1995
ENVISAT	C	All	20–45	30	50–400	ESA	800	100	1998
SRTM	C	HH	20–60	30	60	NIMA/NASA	233	57	2000
PALSAR	L	HH; VV HV; VH	20–55	10–100	70–250	NASDA/MITI	700	98	2002
Light SAR	L	All	20	25–100	50–500	NASA	790	97.7	2003
COSMO-SkyMed ScanSar	X	One and two polarization modes (HH, VV, HV, or VH)	20–59	16–100	100–200	ASI	620	97.8	2007
COSMO-SkyMed StripMap	X		20–59	3–20	30–40	ASI	620	97.8	2007
COSMO-SkyMed SpotLight-2	X		20–59	1	10	ASI	620	97.8	2007
Terra SAR-X StrimMap mode	X	(HH,VV) – (HH/VV, HH/HV, VV/VH)	15–60	1.55–3.21	15–30	DLR-ASTIRUM	514	97.44	2007
Terra SAR-X SpotLight mode	X	(HH,VV) – (HH/VV)	15–60	1.34–3.21	10	DLR-ASTIRUM	514	97.44	2007
Terra SAR-X ScanSar mode	X		15–60	1.55–3.21	100	DLR-ASTIRUM	514	97.44	2007

Durden, 1998; Cloude and Pottier, 1996; Cloude and Pottier, 1997). Some of these models, called target decomposition models, attempt to characterize the backscatter as a sum of elementary scattering mechanisms such as single bounce, double bounce and volume scattering (see Figure 2).

A multiband SAR dataset can be obtained varying several parameters including frequency and polarization. Polarimetric multifrequency models provide increased capacity for target discrimination, classification and analysis, but obviously require more sophisticated processing, including multiband scatter modelling.

The RGB visualization of multiple channels of polarimetric data can help in a visual interpretation, to enhance features of interest and make them recognizable by a trained interpreter. As a simple example, to have a realistic 'look', a RGB can be composed using a HH = red, HV = green and VV = blue channel assignment. This is because water reflections have a higher VV component than HH, whereas vegetation has a higher component than average HV backscatter.

In the civilian sector, diverse spaceborne systems provide polarimetric SAR; see, for example, ERS and ENVISAT (multipolar, multi-incidence angle datasets in C-bands); Radarsat II (multipolar, multifrequency datasets) Terra SAR and CosmoSkymed (for additional details, see http://earth.esa.int/; http://www.ccrs.nrcan.gc.ca/; http://www.dfd.dlr.de/; http://southport.jpl.nasa.gov/).

One limitation of using polarimetric analysis is linked mainly with the unsatisfactory spatial resolution for archaeological features, even if palaeolandscape investigations benefit from this approach.

Incidence angle

The incidence angle refers to the angle between the perpendicular to the imaged surface and the direction of the incident radiation. Backscattering may vary with the incidence angle. The selection of the most appropriate SAR incidence angle is very important for target recognition and mapping. This is because the effects of terrain and surface roughness on SAR backscatter vary with different viewing geometry.

Early experimental tests were carried out by (Ulaby *et al*., 1984) who conducted analyses using the L band (1.1 GHz) on five soils characterized by similar moisture content and different surface roughness conditions. Results from this experience showed that: (i) for rough fields the backscatter was almost independent of the chosen incidence angle; (ii) for smooth fields the backscatter coefficient was very sensitive to near nadir incidence angles. (Elachi and Granger, 1982)

DOI: 10.1002/arp

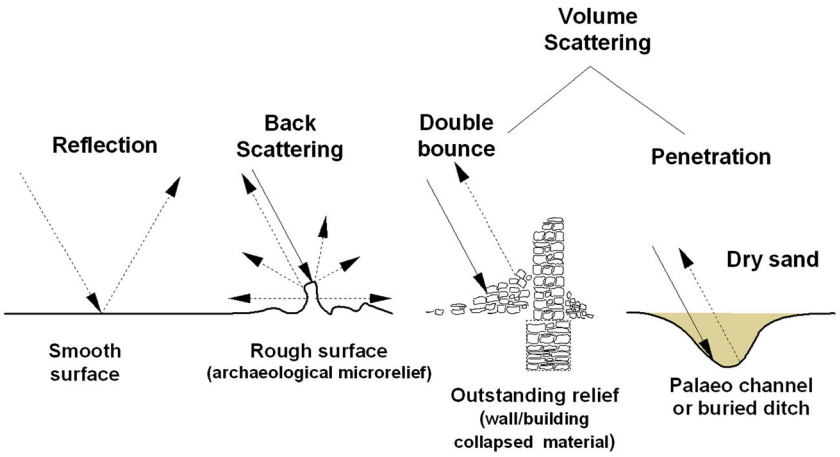

Figure 2. Model of the response of elementary scattering mechanisms: simplified examples are from left to right as single bounce (smooth surface), double bounce (urban settlement remains or upstanding relief) and volume scattering, typically from vegetation, in figure linked to overlapping of the effects of urban settlement remains and soil penetration.

found that the discrimination of palaeo-drainage features was facilitated by large incidence angles (greater than 50°). (Brown *et al.*, 1996), using Radarsat data, showed that larger angles were most useful for detecting emerging archaeological remains.

The SAR viewing geometry is a very significant parameter in the delineation of superficial materials, lithological units and landforms. As an example, (Ahern and Raney, 1993) have shown that the effects of terrain slope on SAR backscatter are significant with different viewing geometry.

Summary

Therefore, the possibility of varying frequency, polarization and incidence angle should enable us to better discriminate some attributes of the target. For example, by varying wavelengths, roughness can be better characterized and quantified, or a smaller incidence angle may be useful for ancient canal mapping enhanced by using VV polarization. Experimental analyses, specifically conducted for archaeological purposes using defined protocols, are needed to obtain systematic information from significant study tests and have the possibility to set up the most useful data processing and devise correct interpretation.

Archaeological investigations based on spaceborne SAR: an overview

Early and past Archaeological investigations conducted during the 1980s

The first SAR system, known as SEASAT, was launched on 28 June 1978 by NASA, for demonstrative studies focused on the oceans; the mission ended on 10 October 1978 due to technical problems.

The 1980s were characterized by intense experimentation in USA. The first shuttle imaging SAR SIR-A was launched in 1981, followed by the launch of SIR-B on June 1984. SIR-B offered significant improvements compared with SIR-A, including for the first time digitally recorded SAR data. Nevertheless, it must be highlighted that SIR-A offered unexpected capabilities in archaeology: in northern Sudan and southern Egypt NASA researchers identified unknown palaeochannels buried under the desert sand (McCauley *et al.*, 1982). This exceptional insight pushed new interest in the use and development of spaceborne SAR technologies.

In the eastern Sahara desert, using SIR-A SAR images, (McCauley *et al.*, 1982) discovered subsurface features (2 m deep) related to defunct rivers and channels. This discovery led to subsequent important implications in the geo-archaeology of prehistoric environments of the region (see also (El-Baz *et al.*, 2007). An old buried river system was also detected using SIR-A data in the Taklamakan desert (Holcomb, 1992; Holcomb and Shingiray, 2007). SIR-C data allowed the detection of a portion of the Great Wall of China (Xinqiao *et al.*, 1997) and to discover the lost City of Ubar (Blom *et al.*, 1984; Blom *et al.*, 1997) in the desert of Oman. In the latter case, to overcome the drawbacks due to low spatial resolution, the discovery of the urban settlements was performed by the identification of the convergence of several ancient roads.

Finally, Mayan ancient irrigation canals and cultivated wetlands were discovered in the Yucatan peninsula using SEASAT data (Adams, 1980; Adams *et al.*, 1981; Pope and Dahlin, 1989; Pope and Dahlin, 1993; Sever, 1998).

DOI: 10.1002/arp

Archaeological investigations conducted during the 1990s

During the 1990s the increasing international interest in spaceborne SAR capabilities was finalized in a number of spaceborne SAR missions operated by the European, Russian, Japanese and Canadian space agencies

In 1991 the European Space Agency (ESA) launched the Earth Remote Sensing Satellite (ERS)-1 and the Russian Space Agency (PKA = RSA) launched the Earth-orbiting satellite ALMAZ-1 (see Table 2). Later ERS-8 was launched in 1995 to collect SAR data similar to that of ERS.

In 1994 NASA put into orbit the Shuttle Endeavour with the first multispectral and multipolarization SAR termed SIR-CIX devised to collect data between latitudes 57"N and 57"S. The SIR-CIX technology was greatly improved in terms of wavelengths and multiple polarizations compared with the previous SIR-A and SIR-B. Three wavebands, L, C and X bands, were simultaneously acquired with multiple polarizations, using multilook angles and varying swaths ranging between 15 and 100 km for the L and between 15 and 40 km for the C and X bands.

In 1995 the Canadian Space Agency (CSA) launched Radarsat the first commercial imaging satellite SAR. In the same year the Russian space agency put into orbit the first spaceborne SAR system exploiting the module PRIRODA of the German Aerospace Center (DLR).

Using the Canadian Radarsat data (Richason and Hritz, 1998) investigated settlements and river systems in the lower Mesopotamian Plain (Nippur archaeological sites in Iraq).

Other discoveries were made in the famous site of Angkor, Cambodia. A vast water management system was identified under tropical forests using SAR images taken from a NASA Space Shuttle (Moore *et al*., 2007). Synthetic aperture radar data were also successfully used in Southeast Asia for archeological exploration. The use of SAR data is mandatory here as the utility of optical imagery is quite limited by the frequent cloud cover and dense forest canopy (Supajanya *et al*., 1994). In northern Thailand, Wara-Aswapati (1994) identified remains of numerous moated cities. Moreover, SAR data also enabled the detection of large canals, which improved the understanding and the identification of the urban area and its chronological evolution (Supajanya *et al*., 1995).

At the end of 1990s other spaceborne SAR missions were operative, icluding ENVISAT by ESA in 1998 and the PALSAR satellite by the Japanese NASDA in 1999.

Archaeological investigations conducted during the 2000s

In 2000 NASA launched the Shuttle SAR Topography Mission (SRTM) designed for interferometric applications between latitudes 60°N and 54°S and for measuring large-scale surface changes. Digital elevation models (DEM) from SRTM data have been and still are one of the most useful and used SAR-based products in archaeology and landscape studies. This is due to the fact that, for the first time, products at 90 m resolution were available free of charge for almost 80% of the Earth's surface. The nearly global availability of the SRTM offers archaeologists the possibility of a prompt virtual survey of large areas for the detection and mapping of huge archaeological features, such as mounds and tells. Several studies were conducted mainly in the Middle East and Near East, using declassified satellite data (Menze and Sherratt, 2006).

Nevertheless, during the past decade, the application of imaging SAR in archaeology has been very limited due to the relatively low spatial resolution of SARs (in L and P bands), the complex interpretation of SAR-based products and the difficulty of accessing low-cost data sets (such as SIR-A, SIR-B and SIR-C). To overcome the low spatial resolution, aerial JPL AirSAR data, along with other remote sensing data sources, were used by (Evans *et al*., 2007) in the urban area of Angkor. The advent of the '2000' generation of spaceborne SAR sensors, such as ENVISAT/ASAR (2002–2012, C band dual), ALOS/ PALSAR (2005–2011, L band), SAR Lupe (2006, X band), CosmoSkymed (2007, X band dual), TerraSAR-X, 2007, X band quad), Radarsat 2 (C band quad, 2007) has provided improved data acquired by multiple polarization modes. The current SAR technology offers a greater flexibility in the selection of the incidence angle range as well as advanced SAR imaging modes such as scanSAR or spotlight.

The launch in 2007 of VHR spaceborne SAR sensors, Italian COSMO-SkyMed and German TerraSAR-X (TSX), offered advanced mapping capability at high-resolution at a scale of 1 m or below (for military applications), even if the SAR was operating in the X band. Both feature three observation modes – namely SpotLight, StripMap and ScanSAR – and are also capable of gathering imagery from different polarizations. Before the availability of VHR SAR, investigations in archaeology were greatly limited by the huge spatial resolution of SARs, which only enabled the survey of upstanding monuments, cultural landscapes, palaeolandscapes and canalization systems. The use of a VHR SAR system coupled with multiple polarization modes can overcome the drawbacks of the early sensors, even though both COSMO-SkyMed and TerraSAR-X have a limited penetration capability.

DOI: 10.1002/arp

The huge archives currently available for the above listed SAR with their user friendly access (see ESA and NASA catalogue) have recently attracted new interests in the use of spaceborne SARs in archaeology, thus providing new vitality in this research field. What is needed in the near future is assessment of the data quality and comparison of performance obtained from the available sensors. This will also require more sophisticated data analysis approaches and tools as well as advanced interpretation techniques, quite different from those currently applied to conventional optical imagery.

This special issue

The challenges and opportunities offered by the current and past SAR with the availability of a huge amount of data stored in historical archives, require great effort aimed at creating a strong interaction among archaeologists, scientists and managers interested in using SAR data for supporting cultural heritage applications. In this cultural framework, the III International EARSEL Workshop 'Advances in Remote Sensing for Archaeology and Cultural Heritage Management', took place in Gent in 2012 and offered the opportunity for young researchers and PhD students to take advantage of a specific course, funded by the European Space Agency, to advance knowledge in the field. Moreover, during the three days of the workshop more than 50 papers were presented and a number of these papers were focused on the use of SAR in archaeology and cultural heritage management.

This special issue of *Archaeological Prospection* is a collection papers selected from the above workshop, focused on archaeological, palaeoenvironmental and historical landscape investigations, based mainly on the use and processing of satellite SAR images. In detail, in this special issue Dore *et al*. investigate the UNESCO Cultural Heritage sites of Samarra (Iraq) and Djebel Barkal archaeological area (Sudan) by means of polarimetric products of the Japanese satellite ALOS PALSAR. Patruno *et al*. focus on the comparison of ALOS (Advanced Land Observing Satellite) PALSAR (Phased Array type L-band Synthetic Aperture SAR) L-band satellite with Radarsat 2 C-band satellite in order to identify the most suitable method for the detection of ground anomalies due to the presence of shallow underground archaeological structures. Linck *et al*., compare Terra SAR data with results of geoSAR survey in order to assess the penetration capability of the SAR X band at a test site of a Roman fortress in Syria. Stewart *et al*. focus on the archaeological site of Pelusium in the northeastern edge of the Nile Delta, Egypt, using PALSAR data. The aim of the investigation was to assess the potential of PALSAR, acquired in various polarimetric modes, to identify buried archaeological structures. Cigna *et al*. use SAR amplitude information from ENVISAT C-band Advanced SAR (ASAR) to analyze the cultural landscape of the Nasca region, southern Peru. The processing method based on SAR amplitude information is also used by Tapete *et al*. to extract the backscattering coefficient ($\sigma 0$) from ENVISA Advanced SAR (ASAR) scenes to investigate ancient pyramids and mounds, and indentify areas affected by looting in the area around Cahuachi, in the Nasca region. Finally, Morison proposes a new scheme for mapping subsurface features with SAR (SubSAR) at large stand-off distances applicable to airborne and satellite measurements.

References

Adams REW. 1980. Swamps, canals, and the locations of Ancient Maya cities. *Antiquity* **54**(212): 206–214.

Adams R, Brown W, Culbert T. 1981. SAR mapping, archeology, and Ancient Maya land use. *Science* **213**: 1457–1463.

Ahern FJ, Raney RK. 1993. An Almaz/ERS-1 comparison demonstrates incidence angle effects in orbital SAR imagery. *Canadian Journal of Remote Sensing* **19**(3): 259–262.

Blom R, Crippen R, Elachi C. 1984. Detection of subsurface features in SEASAT SAR images of Means Valley, Mojave Desert, California. *Geology* **12**: 346–349.

Blom R, Clapp N, Zarins J, Hedges G. 1997. *Space technology and the discovery of the lost city of Ubar*. Paper presented at the IEE Aerospace Conference, Snowmass at Aspen, USA, 1-8 February.

Boerner W-M, Mott H, Lunebug E, *et al*. 1998. Polarimetry in SAR remote sensing: basic and applied concepts. In *Principles and Applications of Imaging SAR, Manual of Remote Sensing*, Vol. 2, Henderson FM, Lewis AJ (eds). John Wiley & Sons: New York; 769–777.

Brown RJ, Brisco B, D'Iorio MA, Prevost C, Ryerson RA, Singhroy V. 1996. RADARSAT Applications: Review of GlobeSAR Program. *Canadian Journal of Remote Sensing* **22**(4): 404–419.

Cloude SR, Pottier E. 1996. A review of target decomposition theorems in SAR polarmetry. *IEEE Transactions on Geoscience and Remote Sensing* **GE-34**(2): 498–518.

Cloude SR, Pottier E. 1997. An entropy based classification scheme for land applications of polarimetric SAR. *IEEE Transactions on Geoscience and Remote Sensing* **GE-35**(1): 68–78

Elachi C, Granger J. 1982. Spaceborne imaging SARs probe 'in depth'. *IEEE Spectrum* **19**: 24–29.

El-Baz F, Robinson CA, Al-Saud TSM. 2007. SAR images in geoarchaeology of eastern Sahara. In *Remote Sensing in Archaeology*, Wisemann J, El Baz F (eds). Springer-Verlag: Berlin; 47–70.

Evans DL, Farr TG, Van Zyl JJ, Zebker H. 1988. SAR polarimetry: analysis tools and applications. *IEEE Transactions on Geoscience and Remote Sensing* **26**(6): 774–789.

DOI: 10.1002/arp

Evans D, Pottier C, Fletcher R, *et al*. 2007. A comprehensive archaeological map of the world's largest preindustrial settlement complex at Angkor, Cambodia. *Proceedings of the National Academy of Sciences of the United States of America* **104**(36): 4277–4282.
Freeman A, Durden SL. 1992. A three-component scattering model to describe polarimetric SAR data. *Proceedings of SPIE* **1748**; 213–225.
Freeman A, Durden SL 1998. A three-component scattering model for polarimetric SAR data. *IEEE Transactions on Geoscience and Remote Sensing* **36**: 963–973.
Holcomb DW. 1992. Shuttle imaging SAR and archaeological survey in China's Taklamakan Desert. *Journal of Field Archaeology* **19**(1): 129–138.
Holcomb DH, Shingiray IL. 2007. Imaging SAR in archaeological investigations: an image processing perspective. In *Remote Sensing in Archaeology*, Wisemann J, El Baz F (eds). Springer-Verlag: Berlin; 11–45.
McCauley JF, Schaber GG, Breed CS, *et al*. 1982. Subsurface valleys and geoarchaeology of the eastern Sahara revealed by Shuttle SAR. *Science* **218**: 1004–1020.
Menze BH, Sherratt AG. 2006. Detection of ancient settlement mounds: archaeological survey based on the SRTM terrain model. *Photogrammetric Engineering and Remote Sensing* **72**: 321–327.
Moore E, Freeman T, Hensley S. 2007. Spaceborne and airborne SAR at Angkor. Introducing new technology to the ancient site. In *Remote Sensing in Archaeology*, Wisemann J, El Baz F (eds). Springer-Verlag: Berlin; 185–216.
Pope KO, Dahlin BH. 1989. Ancient Maya wetland agriculture: new insights from ecological and remote sensing research. *Journal of Field Archaeology* **16**: 87–106.
Pope KO, Dahlin BH. 1993 SAR detection and ecology of Ancient Maya canal systems – reply to Adams *et al*. *Journal of Field Archaeology* **20**: 379–383.
Richason III FB, Hritz C. 1998. The use of digitally enhanced Radarsat SAR imagery in the interpretation of archaeological sites in the Nippur, Iraq, area of the Lower Mesopotamian Plain. *Proceedings of the International Conference on Remote Sensing in Archaeology from Spacecraft, Aircraft, on Land and in the Deep Sea*, Boston University, Boston, April 16–19.
Sever TL. 1998. Validating prehistoric and current social phenomena upon the landscape of the Peten, Guatemala. In *People and Pixels*, Liverman D, Moran EF, Rindfuss RR, Stern PC (eds). National Academy Press: Washington, DC; 145–163.
Supajanya T, Vichapan K, Chaleamlarp S, Srisuchat T, Srisuchat A, Pornpraseertchai J. 1995. Archaeo-geomorphic feature observation using SAR imagery in Sukhothai, the ancient capital city of Thailand. *Proceedings of the Second Asia Regional GlobeSAR Workshop*, Beijing, 9–12 October.
Supajanya T, Vichapan K, Chaleamlarp S, Srisuchat T, Srisuchat A, Pornpraseertchai J. 1994. Sukhothai and its hydraulic past, a demonstrative project for Radarsat. *Proceedings of the First Asia Regional GlobeSAR Workshop*, Bangkok, Thailand, 28 November to 2 December; 110–118.
Ulaby FT, Allen RK, Eger G, Kanemasu E. 1984. Relating microwave backscattering to leaf area index. *Remote Sensing of Environment* **14**: 113–133.
Wara-Aswapati P. 1994. Preliminary study of airborne SAR for land identification in north-eastern Thailand. *Proceedings of the First Asia Regional GlobeSAR Workshop*, Bangkok, Thailand, 28 November to 2 December; 46–52.
Xinqiao L, Huadong G, Yun S. 1997. Detection of the Great Wall using SIR-C data in north-western China. Geoscience and remote sensing. *IGARSS '97. Remote Sensing – A scientific Vision for Sustainable Development IEEE International* **1**: 50–52.

Rosa Lasaponara
Institute of Methodologies for Environmental Analysis, National Research Council, C.da S. LojaI-85050 Tito ScaloPotenza, Italy.
Italian Mission of Heritage Conservation and Archaeogeophysics in Peru.

Nicola Masini
Institute for Archaeological and Monumental Heritage, National Research Council, C.da S. LojaI-85050 Tito ScaloPotenza, Italy.
Italian Mission of Heritage Conservation and Archaeogeophysics in Peru.

DOI: 10.1002/arp